IV. Lateral Excitation of Thickness Modes

Lateral excitation is the second canonical form of excitation of thickness modes. It has been the subject of recent interest (207-215), although use was made of it by Atanasoff & Hart (44), referenced in Cady's book (160). Also, excitation by an electric field lateral to the wave propagation direction is often used with vibrators in the form of bars. We have chosen the name given in the chapter title, (abbreviated as LETM) to characterize this type of excitation. As much confusion arises from other names that abound in the literature, it seems to us least ambiguous in this form.

In this chapter we will parallel the treatment given the TETM case in the last chapter, considering first a traction-free plate analytically, then obtaining a network that realizes the electrical port immittance. After this, the seven-port admittance matrix for the normal coordinate system is derived, analytically, and realized as a network, which is shown to be a true analog of the acoustic problem.

Our efforts are aided by similarities that this problem shares with the first (TETM) canonical form, so that certain of the properties will be recognized by inspection, such as the symmetry of the admittance matrix, and the possibility of obtaining additional matrix coefficients by permuting the mode index number. These features will therefore be discussed briefly only.

Concerning the analytical portion, there seems not to be any published material relating directly to the derivation as we shall give it. Schweppe (215) consideres two modes driven by LETM, but limits the

discussion to ceramics, (class 6mm), while the other publications treat of only one mode, or of a number of modes each of which is uncoupled to the others at the boundaries, in the manner of Lawson's TETM paper (61). What we shall give for the traction-free plate is patterned after Tiersten's treatment (216a,b).

A. Single-Plate Crystal Resonator, Traction-Free.

1. The plate under consideration is presumed to be laterally unbounded and of thickness 2h; the upper and lower surfaces at $x_3 = +h$ and $-h$, respectively, are further presumed to have no mechanical surface-tractions applied. A uniform electric field is applied in a direction perpendicular to the thickness coordinate. Without loss in generality, we take the field direction as the negative x_1 axis. This specification of a lateral field now requires the lateral coordinates to be distinguished, and the matter tensors specifying the phenomenological elastic, piezoelectric and dielectric properties have to be referred from the X,Y,Z system to the new x_i system, now established. In the TETM case, only such components as were referred to x_3 were required.

The mechanism for establishing the impressed electric field is not of interest to us; we suppose it to be set up by an electrode arrangement sufficiently far removed from the section of plate we focus our attention upon that any effects other than those arising from an assumed uniform lateral field, are negligible. The time factor, $\exp(j\omega t)$, is suppressed. Figure 16 shows a section of the plate.

At the plate boundaries, the conditions to be satisfied are

$$T_{3j} = 0, \qquad \text{at } x_3 = \pm h, \tag{3.1}$$

and

$$D_3 = 0, \qquad \text{at } x_3 = \pm h. \tag{4.1}$$

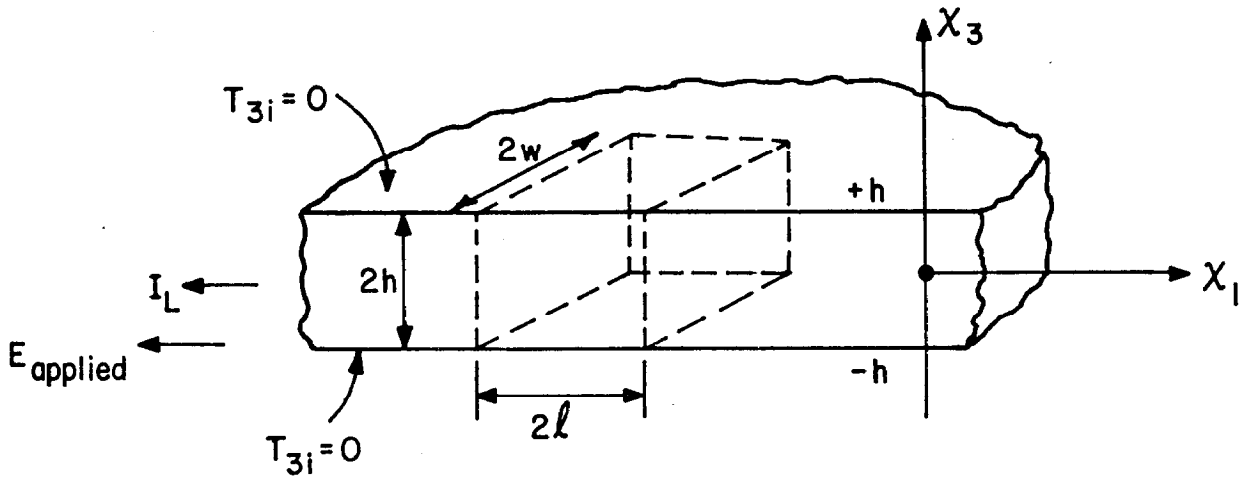

FIG. 16. UNBOUNDED, TRACTION - FREE, PIEZOELECTRIC PLATE. LATERAL EXCITATION OF THICKNESS MODES.

The mechanical condition (3.1) is the same as in the TETM case, and we also have, as a consequence,

$$T_{3i}^{\circ} = 0 , \qquad at\ x_3 = \pm h . \tag{3.3}$$

The condition (4.1) replaces (3.2). D_3 must still be a constant throughout the plate, and, because of (4.1), that constant must be zero, however, it cannot be shown from (2.20) because we shall find that the applied electric field modifies this expression. The assumption, in Chapter II, of no lateral field variations was valid both in Chapter III and here because E(applied) is uniform. This implies a laterally varying potential, however, which we take as

$$\varphi = (e_{3k3}/\epsilon_{33}^{S})\, u_k + a_3 x_3 + a_1 x_1 + b_3 , \tag{4.2}$$

using (2.17) as a guide; (4.2) satisfies the completely general (2.16).

If we take the applied field to point in the negative x_1 direction, as the applied TETM field pointed in the negative x_3 direction, it follows that a_1 is positive in value. From (2.4), the positive-directed electric field in the x_1 direction is called E_1, and (4.2) gives its value as

$$E_1 = -a_1 = -E(applied) . \tag{4.3}$$

This added term must be included when (2.5) is written out. We will take E_1 as a given value which is fixed for the problem. It is seen that E_1 by itself satisfies the electrical boundary condition that the tangential component of the field shall be continuous across the boundaries, so the field in the x_1 direction, external to the crystal,

is likewise equal to E_1 .

When (2.5) is written out, we get, instead of (2.13),

$$T_{3j} = c^{E}_{3jk3}\, u_{k,3} + e_{33j}\, \varphi_{,3} - e_{13j} E_1 \; ; \tag{4.4}$$

and, similarly, (2.6) now gives

$$D_3 = e_{3k3}\, u_{k,3} - \epsilon^{S}_{33}\, \varphi_{,3} + \epsilon^{S}_{31} E_1 \; , \tag{4.5}$$

instead of (2.14). In the quantities e_{13j} and ϵ^{S}_{31} we have the first appearance of components of the material tensors referring to a lateral axis.

From (4.2) we have

$$\varphi_{,3} = (e_{3k3} / \epsilon^{S}_{33})\, u_{k,3} + a_3 \; , \tag{4.6}$$

and when this is inserted into (4.5), D_3 becomes

$$D_3 = - \epsilon^{S}_{33}\, a_3 + \epsilon^{S}_{31} E_1 \; , \tag{4.7}$$

but, as (4.1) makes D_3 equal to zero, arising from the fact that no current can now flow in the x_3 direction, we are able to evaluate a_3 :

$$a_3 = + (\epsilon^{S}_{31} / \epsilon^{S}_{33})\, E_1 \; . \tag{4.8}$$

Substitution of (4.6) and (4.8) into (4.4) gives

$$T_{3j} = \bar{c}_{3jk3}\, u_{k,3} - \bar{e}_{13j} E_1 \; , \tag{4.9}$$

where

$$\bar{c}_{3jk3} = c^{E}_{3jk3} + e_{33j}\, e_{3k3} / \epsilon^{S}_{33} \tag{2.19}$$

are the same piezoelectrically stiffened elastic stiffnesses encountered in Chapter II.

The quantities $\underline{e}_{13j}$ are given by

$$\underline{e}_{13j} = e_{13j} - (\epsilon'_{31}/\epsilon'_{33})\, e_{33j} \,. \tag{4.10}$$

We will need D_1 in order to determine the current and admittance of this configuration. We use (2.6) to obtain

$$D_1 = e_{1k3}\, u_{k,3} - \epsilon'_{13}\, \varphi_{,3} + \epsilon'_{11} E_1 \,, \tag{4.11}$$

where (2.4) has also been used. When (4.6) and (4.8) are put into (4.11), we arrive at

$$D_1 = \underline{e}_{1k3}\, u_{k,3} + \underline{\epsilon}_{11} E_1 \,. \tag{4.12}$$

In this expression $\underline{e}_{1k3}$ equals the following

$$\underline{e}_{1k3} = e_{1k3} - (\epsilon'_{31}/\epsilon'_{33})\, e_{3k3} \,, \tag{4.13}$$

and $\underline{\epsilon}_{11}$ is

$$\underline{\epsilon}_{11} = \epsilon'_{11} - \epsilon'_{13}\, \epsilon'_{31}/\epsilon'_{33} \,. \tag{4.14}$$

Because of the symmetry of e_{kij} to an interchange of the last two indices, and because ϵ'_{ik} are likewise symmetric, (4.13) is the same as (4.10), and (4.14) can be written

$$\underline{\epsilon}_{11} = \epsilon'_{11} - (\epsilon'_{13})^2/\epsilon'_{33} \,. \tag{4.15}$$

2. We now transform to normal coordinates to uncouple the motions. In the transformed system we have

$$T^{\circ}_{3i} = c^{(i)}\, u^{\circ}_{i,3} - \underline{e}^{\circ}_{13i} E_1 \,, \tag{4.16}$$

and

$$D_1 = \underline{e}^{\circ}_{1i3}\, u^{\circ}_{i,3} + \underline{\epsilon}_{11} E_1 . \qquad (4.17)$$

Equation (4.16) is obtained as in (2.35)-(2.38), and (4.17) comes from (4.12) and (2.40), where

$$\underline{e}^{\circ}_{13i} = e^{\circ}_{13i} - (\epsilon^{S}_{31} / \epsilon^{S}_{33})\, e^{\circ}_{33i} , \qquad (4.18)$$

and $\underline{\epsilon}_{11}$ is given by (4.15).

The wave equation (2.39) must, of course, additionally be satisfied by any solution u°_i that satisfies (4.16) and (3.3). Regarding the symmetry of the traction-free plate, we take the same solution as for the TETM case:

$$u^{\circ}_i = U_i \sin x^{(i)} x_3 , \qquad (3.4)$$

which satisfied (2.39), and use it with (4.16) and (3.3):

$$\begin{aligned} T^{\circ}_{3i} &= c^{(i)} u^{\circ}_{i,3} - \underline{e}^{\circ}_{13i} E_1 \\ &= c^{(i)} x^{(i)} U_i \cos x^{(i)} h - \underline{e}^{\circ}_{13i} E_1 \\ &= 0 \qquad \text{at} \quad x_3 = \pm h , \end{aligned} \qquad (4.16)$$

hence

$$U_i = \frac{+\ \underline{e}^{\circ}_{13i} E_1}{c^{(i)} x^{(i)} \cos x^{(i)} h} . \qquad (4.19)$$

Therefore,

$$T^{\circ}_{3i} = - \underline{e}^{\circ}_{13i} E_1 \left\{ 1 - \frac{\cos x^{(i)} x_3}{\cos x^{(i)} h} \right\} , \qquad (4.20)$$

which is the same form as (3.8) for the TETM case, while

$$u_i^\circ = \frac{\underline{e}_{13i}^\circ E_1 \sin x^{(i)} x_3}{c^{(i)} x^{(i)} \cos x^{(i)} h} , \tag{4.21}$$

which is to be compared with the corresponding (3.9) for TEIM.

Now we can evaluate D_1 by putting (4.21) into (4.17), yielding

$$D_1 = \left\{ \underline{\epsilon}_{11} + \frac{\underline{e}_{13i}^\circ \underline{e}_{1i3}^\circ}{c^{(i)}} \cdot \frac{\cos x^{(i)} x_3}{\cos x^{(i)} h} \right\} E_1 , \tag{4.22}$$

so that D_1 is a function of x_3, instead of being a constant, as is D_3. To obtain the x_1-directed current, we must integrate. We take a portion of area normal to x_1, of width $2w$,

$$A_L = (2h)(2w) , \tag{4.23}$$

and find the current which it intercepts from

$$I_L = -j\omega (2w) \int_{-h}^{+h} D_1 \, dx_3 , \tag{4.24}$$

where the negative sign arises in the same manner as in the TEIM case. With D_1 from (4.22) inserted into (4.24), and the integration carried out, one finds, for I_L,

$$I_L = -j\omega (2w) E_1 \left\{ 2h \, \underline{\epsilon}_{11} + \sum_{i=1}^{3} \frac{2 \underline{e}_{13i}^\circ \underline{e}_{1i3}^\circ}{c^{(i)} x^{(i)}} \tan x^{(i)} h \right\} . \tag{4.25}$$

Defining $\underline{k}^{(i)}$, the LETM coupling factor for mode (i), by

$$\left(\underline{k}^{(i)}\right)^2 = \frac{\underline{e}_{13i}^\circ \underline{e}_{1i3}^\circ}{\underline{\epsilon}_{11} c^{(i)}} , \quad \text{(no sum)} \tag{4.26}$$

allows (4.25) to be expressed as

$$I_L = -j\omega(2w)(2h)E_1 \in_{11} \left\{ 1 + \sum_{i=1}^{3} \left(\underline{k}^{(i)}\right)^2 \frac{\tan \chi^{(i)} h}{\chi^{(i)} h} \right\}. \tag{4.27}$$

We now have an expression for the x_1-directed current arising as a result of the plate vibrations responding to the time-harmonic impressed electric field E_1. In order to arrive at an equivalent network representation, we arrange our definition of admittance to take into account an elemental portion of the plate. This was done in the TETM case, where a portion of area of size A was selected and the current intercepted by it was found. For the TETM unbounded plate as a whole, the total current would itself be unbounded, so the calculation is a form of normalization, and the whole problem then appears as a sum of elemental plate portions all connected electrically in parallel. For the LETM case we again make a normalization, but this time it is more appropriate to consider the elemental sections as being electrically in series. We determine the admittance on this basis. To do this we first consider that the imposed field E_1 arises from a potential difference in the lateral direction equal to $(-E_1 (2\ell))$, where 2ℓ is an arbitrary length in the x_1 direction. See Fig. 16. Then the input admittance Y_{in} (LETM) would be, in the same manner as (3.13),

$$Y_{in}\ (\text{LETM}) = -I_L / (2\ell E_1) . \tag{4.28}$$

The capacitance between two plates of area A_L, separated by distance 2ℓ,

in a medium of permittivity $\underline{\epsilon}_{11}$, is

$$\underline{C}_0 = \underline{\epsilon}_{11} A_L / (2\ell) , \tag{4.29}$$

so (4.28) can be put into the form

$$Y_{in\ (LETM)} = +j\omega \underline{C}_0 \left\{ 1 + \sum_{i=1}^{3} \left(\underline{k}^{(i)}\right)^2 \frac{\tan \varkappa^{(i)} h}{\varkappa^{(i)} h} \right\} . \tag{4.30}$$

It will be seen that the entire plate appears as an assembly of elemental areas in series such as we have considered. In the final result, (4.30), the tranverse length (2ℓ) does not appear, but appears instead in the tranverse capacitance $\underline{Co}$.

B. Network Synthesis of Y_{in} (LETM).

1. The task of performing a one-port synthesis of (4.30) is greatly simplified by the work of Chapter III for the TETM case, and by the simpler nature of (4.30), compared with (3.15). We see, first of all, that Y_{in} (LETM) consists of four admittances in parallel, one of which is simply realized by a capacitor of value $\underline{Co}$. What then remains is nothing more than Y_{TL} from (3.16), with a suitable substitution of $\underline{Co}$ for Co and $\underline{k}^{(i)}$ for $k^{(i)}$. But we know that Y_{TL} in (3.16) is realized by the parallel combination of three networks of the form of Fig. 9, so we are led immediately to the circuit of Fig. 17.

It is to be emphasized that the $\varkappa^{(i)}$ appearing in (3.15) and (4.30) are identical; both come from solving the same wave equation, (2.39), where the $c^{(i)}$ are the same for both, coming from (2.19) in each case. That is to say, the same stiffened elastic constants determine the wave

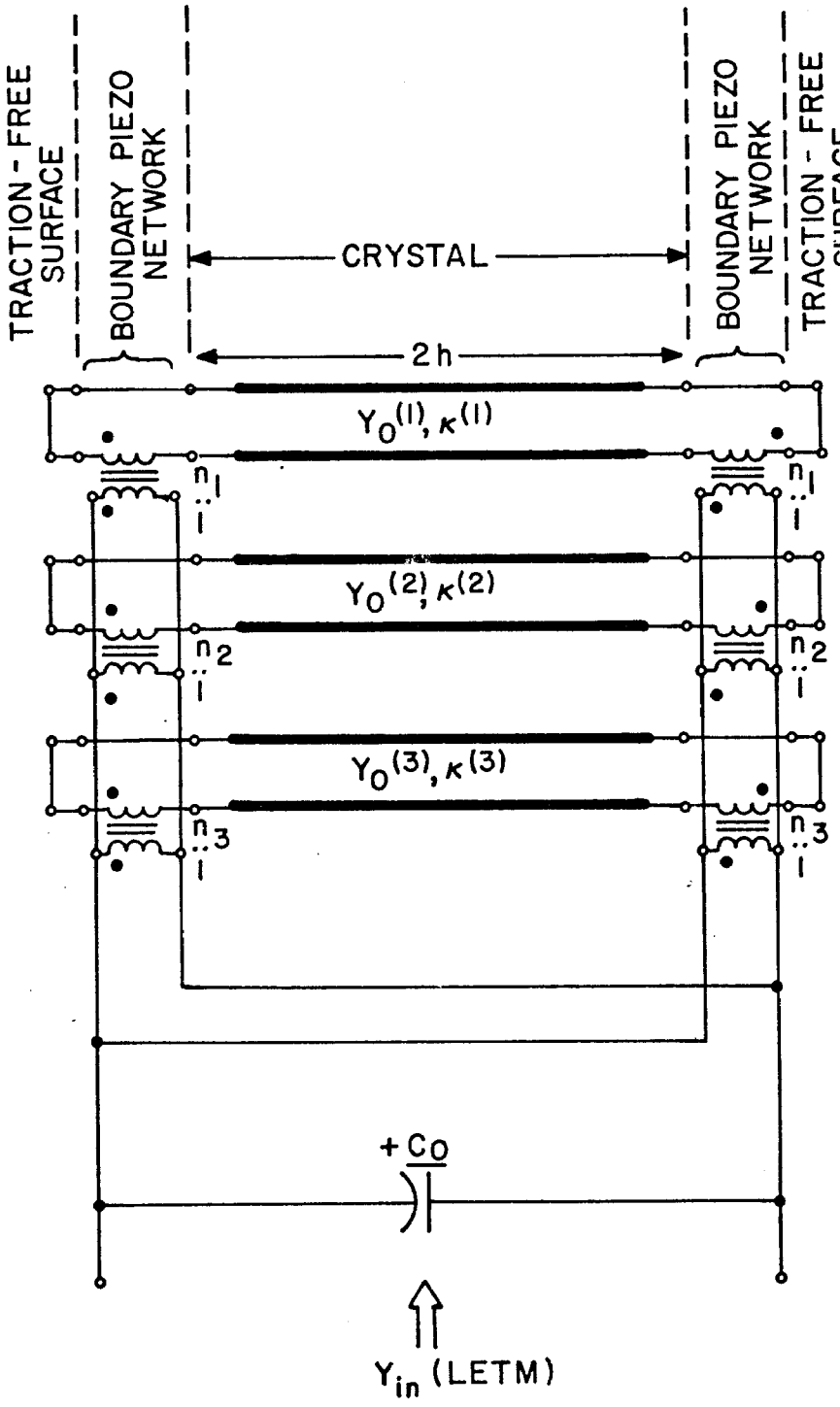

FIG. 17. EQUIVALENT NETWORK ANALOG REPRESENTATION OF TRACTION-FREE PLATE, LETM.

propagation velocities on the transmission lines in both the TETM and LETM cases, and these velocities are the same as for the case of an unbounded medium. The differences that exist come from the presence or absence of the negative capacitance, and, of course, the fact that Co refers to a capacitor whose plates are normal to x_3 while the plates of $\underline{Co}$ are normal to the x_1 axis. The piezoelectric transformer turns ratios are different in the two cases and this is an important fact, because here lies the key to the misunderstanding about "stiffened modes" and "unstiffened modes" which prevails in the literature. It should also be noted that the piezo-transformers have been located at the boundary, as with the TETM case. It cannot be shown from a one-port synthesis that this is indeed where they belong, but this will be shown subsequently, as was done in Chapter III.

In Fig. 17, as in our previous work, we have used

$$Y_o^{(i)} = 1/(A\rho v^{(i)}) , \tag{4.31}$$

$$\chi^{(i)} = \omega / v^{(i)} , \tag{2.45}$$

whereupon the piezoelectric transformer turns ratios, n_i become

$$n_i = \frac{+A_L \, \hat{e}^{\circ}_{13i}}{2h} , \tag{4.32}$$

with the transformer dots as shown. Notice that the area factor in (4.31) refers to the plane normal to x_3, while the factor in (4.32) has a normal in the direction of x_1. This is because $Y_o^{(i)}$ refers

to the transmission lines which extend along x_3, whereas the transformer turns ratios depend upon the cross sectional area which intercepts the current flow in either the TETM or LETM case. For the TETM case, the area factor in (3.17) is just A, whose normal is along x_3, the direction of the current, while for LETM, the current is along x_1 so (4.32) contains the quantity A_L, defined in (4.23), with normal along x_1.

2. We now make some remarks with reference to the literature; in particular, we review some past work in the light of our general results, so far, for the LETM plate.

The presence or absence of the negative capacitor is the first indication of the type of excitation; the LETM electrical input circuit consists of only a single shunt capacitor. This separation of the input circuit from the portion representing the vibration was mentioned in connection with Schüssler's paper (143).

In Schweppe's paper (215) he derives the equivalent of (4.30) for two modes in a ceramic plate. He shows that by means of a variation in the angle which the applied field makes in the lateral plane, which is the same as rotating the crystallographic XYZ axes about our x_3, with respect to our x_1 axis, the amplitudes of the two modes which he treats can be altered with respect to each other. Such a device could be used to reduce the number of resonators in a filter; the idea has been applied to the shear and quasi-shear modes in a rotated Y-cut quartz plate (214a,b).

The case of one mode being excited by a lateral field was first treated by Mason (130) in 1939, where the motion of a bar was analyzed.

He obtained the resonance frequencies from the harmonically-related roots of

$$\tan \varkappa h = \infty \,, \tag{4.33}$$

and the non-harmonically-related antiresonant frequencies from the roots of

$$\tan \varkappa h = - \varkappa h \,(1-k^2)/k^2 \,. \tag{4.34}$$

One can see that the TETM antiresonances coincide with the LETM resonances. For the situation where only one mode of either is driven, the construction for finding the roots is given nicely by Schüssler (143); Tiersten (64) first gave the TETM construction, and the other follows from it.

From the differences between the roots of (3.19), (3.20) and (4.33), (4.34) the electromechanical coupling factors may be determined (141). The differences which arise from the types of excitation, TETM and LETM, can also be used to explain the finding of Bechmann (208,210) that a production version of a high precision quartz TETM vibrator, when converted to LETM operation, had its fundamental resonance frequency shifted upward slightly. Viewed as a consequence of the change in conditions from (3.20) to (4.33), it is seen to be an effect due the coupling coefficient, which may be found from his data.

Just as with the TETM case, the solution (4.30) is exact, and the realization of Fig. 17 also exactly realizes (4.30) so the network is valid for transient studies, and can additionally be used down to DC. At DC the network degenerates to a simple parallel combination of $\underline{C}o$ and three capacitors of value $\underline{C}o(\underline{k}^{(i)})^2$. Notice that we

cannot say anything like (3.22) now, since the input capacitance of such a circuit is always positive for real values $\underline{k}^{(i)}$. If, however, we wish to make a comparison between the two cases TETM and LETM in the DC limit, supposing that Co = $\underline{Co}$, then we would have identical input capacitances in each case providing

$$\frac{1}{1 - \sum_{p=1}^{3} (k^{(p)})^2} = 1 + \sum_{i=1}^{3} (\underline{k}^{(i)})^2 , \qquad (4.35)$$

or in the case of only one mode of each type,

$$\frac{1}{1 - k^2} = 1 + \underline{k}^2 , \qquad (4.36)$$

which leads immediately to

$$\underline{k}^2 = \frac{k^2}{1 - k^2} , \qquad (4.37)$$

or, alternatively

$$k^2 = \frac{\underline{k}^2}{1 + \underline{k}^2} . \qquad (4.38)$$

An identical relationship, (4.36)-(4.38), is found by Bechmann (137), between one-dimensional coupling factors, from an entirely different point of view.

Coming back to (4.34), the quantity $(1-k^2)/k^2$ can be replaced simply by the LETM coupling factor $\underline{k}^2$ from (4.37), so that (4.34) and (3.20) differ now only by the sign of $\varkappa h$.

In the single-mode case, we noted in Chapter I, in connection

with Mason's exact 1939 LETM network (130), that it was equivalent to Butterworth's circuit (129). It is instructive to think of these two alternates in connection with the normal-coordinate transformation we introduced in Chapter II. We saw that this transformation in the physical problem allowed us to put the network results into transmission-line form, that is, the transmission lines represent the three normal modes of the system.

Guillemin (217) discusses normal-coordinate transformations applied to circuits and shows that such a transformation leads to network realizations as Foster forms. Butterworth's 1915 circuit, which incidentally, predates Foster's work (217) is just one Foster form, wherein the normal coordinates are placed in evidence, and the method for doing this, starting from the transmission line, is the partial-fractions expansion, as was used by Marutake (144,145).

3. Having worked both traction-free problems, we are now in a position to consider the "stiffened" and "unstiffened" question.

A distinction has grown up in the literature between the TETM case (also the corresponding case for a bar or rod), and the LETM case (similarly for bar or rod), where a mode of the former is called a "stiffened mode," while a mode of the latter is referred to as an "unstiffened mode." That there is a distinction to be made is certainly true; the terminology, however, is unfortunate, and this is not merely a cavil.

The origin for the terms doubtlessly lies in the fact that for most of the popularly used substances and cuts, it arises that the TETM situation produces a driven mode whose phase velocity depends upon stiffened elastic constants $\bar{c}_{3j\,k3}$, (see (2.19)), while the

LETM situation produces a driven mode whose phase velocity depends only upon the unstiffened values $\mathcal{C}^{E}_{3jk3}$.

Our general results permit the following observations. The TETM and LETM cases are distinguished by the presence or absence of a negative capacitor, by the difference in orientation of Co and $\underline{Co}$ and by the quantities which enter the piezo-transformer turns ratios. The transmission lines are identical for both cases. This means that, in general, both TETM and LETM will drive a "stiffened mode."

As we shall show a TETM-driven mode must be a "stiffened mode" and a "stiffened mode" must be TETM-drivable, whereas a LETM-driven mode may be a "stiffened mode" or not, and a "stiffened mode" may or not be drivable by LETM; likewise, an "unstiffened mode" may or may not be LETM-drivable.

This is seen as follows. The criterion of whether a mode can be driven or not, is whether the corresponding piezo transformer, connected to that modal transmission line, has a finite or zero turns ratio. This is determined by the proper transformed piezoelectric constant; from (3.17), this constant is e°_{33i} for TETM and, from (4.32), $\underline{e}^{\circ}_{13i}$ for LETM.

The effective stiffness determining the velocity and wavenumber $\varkappa^{(i)}$, for transmission line (i) is $c^{(i)}$. We may relate this to $\bar{\mathcal{C}}_{3jk3}$ as follows: starting from (2.19), which is

$$\bar{\mathcal{C}}_{3jk3} = \mathcal{C}^{E}_{3jk3} + e_{33j}\, e_{3k3} / \epsilon^{S}_{33} , \qquad (2.19)$$

multiply through by $\beta^{(i)}_{j}$ and apply (2.34) and (2.29) to get

$$\mathcal{C}^{(i)}\, \delta_{kj}\, \beta^{(i)}_{j} = \mathcal{C}^{E}_{3jk3}\, \beta^{(i)}_{j} + e^{\circ}_{33i}\, e_{3k3} / \epsilon^{S}_{33} . \qquad (4.39)$$

Now multiply through by $\beta_k^{(i)}$ and apply (2.26) and (2.29) which gives

$$c^{(i)} = \beta_j^{(i)} c_{3jk3}^{E} \beta_k^{(i)} + e_{33i}^{\circ} e_{3i3}^{\circ} / \epsilon_{33}^{S} . \qquad (4.40)$$

By the use of (3.7), this can be written in other equivalent forms, such as

$$c^{(i)} = \beta_j^{(i)} c_{3jk3}^{E} \beta_k^{(i)} / (1 - (k^{(i)})^2) . \qquad (4.41)$$

It is enough for us to see, from (4.40), that the eigenvalue $c^{(i)}$ depends upon e_{33i}° for its piezoelectric stiffening, and this is the quantity that determines the turns ratios for the TETM case. This proves that a TETM-driven mode must be a "stiffened mode" and conversely.

In the case of LETM, it is obvious that e_{13i}° may be finite while e_{33i}° is zero because they are independent of each other. This would make the second term on the right hand side of (4.40) zero and $c^{(i)}$ would be determined by the c_{3i3j}^{E} only, without any piezoelectric stiffening; hence, in this instance, the LETM-driven mode is an "unstiffened mode." But if e_{33i}° is finite, then $c^{(i)}$ must have a piezoelectric stiffening term; so, by (4.18), if furthermore e_{13i}° and/or ϵ_{31}^{S} are/is also finite, then this "stiffened mode" is LETM-drivable, in contradiction to the usual notions prevailing in the literature. The general circumstances under which a mode is excitable or not are given in Fig. 18.

4. Let us go on now to the simplification of Fig. 17. The same arguments we gave in Section III B hold good here. Briefly, the symmetrical excitation of the transmission lines guarantees that the centers thereof are nodes of displacement, which is

e°_{33i} → / e°_{13i} ↓		FINITE	ZERO
		$C^{(i)}$ STIFFENED	$C^{(i)}$ UNSTIFFENED
FINITE	$\epsilon^{S}_{13}=0$	TETM LETM	——— LETM
	$\epsilon^{S}_{13}\neq 0$	TETM LETM	——— LETM
ZERO	$\epsilon^{S}_{13}=0$	TETM ———	——— ———
	$\epsilon^{S}_{13}\neq 0$	TETM LETM	——— ———

FIG. 18. CONDITIONS FOR DRIVING MODES BY TETM & LETM.

to say, of mechanical current. The same thing is, of course, to be seen from (3.4) as well. Therefore the transmission lines may be opened at this point. The two lines, each now of length h, belonging to mode (i), are then in parallel and may be replaced by one line of twice the characteristic admittance.

There thus results three lines on a bisected basis. In the resulting figure, Fig. 19, one has a circuit very much like that of Fig. 11, save for the absence of the negative capacitor, the replacement of Co by $\underline{Co}$ and the substitution of (4.32) for (3.17) in the turns ratios.

The establishment of the seven-port electromechanical admittance matrix will concern us next.

C. The LETM Plate Electromechanical Admittance Matrix.

We shall now continue in the fashion of Chapter III to establish the seven-port immittance matrix appropriate to the LETM problem. It will turn out that LETM and TETM are very nearly duals of one another, and that, just as the negative capacitor found to be present in the TETM case made it advantageous to work with the impedance matrix then, it will prove to our advantage to use the admittance formulation now.

It will be recalled that evaluation of the impedance matrix elements involved placing open circuits at all ports, and this had the result, in the TETM situation, that when port (7°) was opened, the negative capacitance, added to the positive, produced a short across the piezo-transformers which decoupled the transmission lines. This rendered the impedances easy to determine, whereas the admittance matrix elements, which involve short circuits at

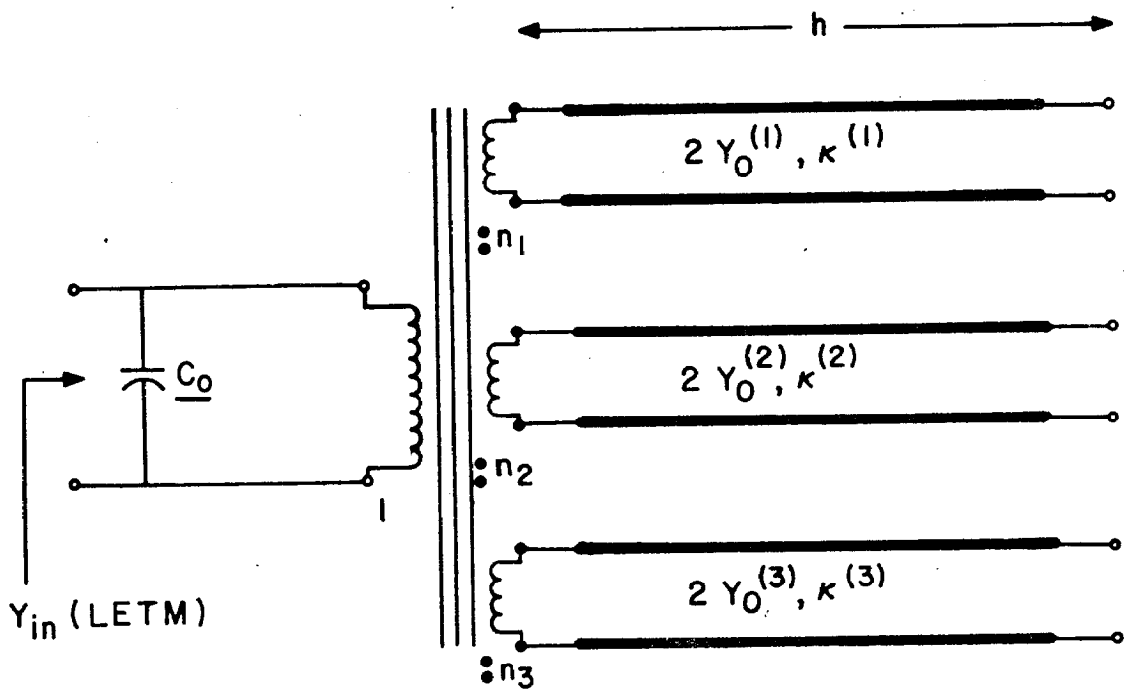

FIG. 19. EXACT EQUIVALENT NETWORK FOR TRACTION-FREE PLATE, LETM. BISECTED BASIS.

all ports, would have had the effect of placing the negative Co across the transformers, and the transmission lines would have remained coupled.

In the present instance, where the negative capacitance is absent, a short at port (7°) reflects directly upon the transformers to produce the desired decoupling. Hence, we use the admittance formulation to express the LETM results.

This time we will start with the plate equations, after which the network realization will be obtained.

1. We again choose, for our definitions of port voltages and currents, equations (3.35)-(3.40). By definition, the admittance element $y^{o}_{\pi\xi}$ is obtained from

$$y^{\circ}_{\pi\xi} = I^{\circ}_{\pi} / V^{\circ}_{\xi}, \tag{4.42}$$

with all voltages equal to zero but V^{o}_{ξ}. This means physically that the plate will be completely traction-free when y^{o}_{77} is determined and have only one component of transformed stress applied, and that to only one side when the other admittance elements are determined.

Thus the conditions required to obtain y°_{77} we have already met when the traction-free plate was analyzed in Section IVA, and y^{o}_{77} is recognized as being equal to Y_{in} (LETM), which is given in (4.30). It remains for us to obtain the components of self and mutual mechanical admittance, and mutual electromechanical admittance.

The same argument that led to chosing (3.45) is applicable here, except, as we wish to force with a single non-zero voltage, rather than with a current, we take instead

$$T^{\circ}_{3i} = G_i \sin \alpha^{(i)}(h \pm x_3). \tag{4.43}$$

When the self and mutual mechanical admittances are to be determined, the electrical port must be shorted. This leads to setting E_1 equal to zero in (4.16), which then reads

$$T_{3i}^{o} = c^{(i)} u_{i,3}^{o} \quad . \tag{4.44}$$

With the assumed form of T_{3i}^{o} in (4.43), the transformed displacements become

$$u_i^{o} = \frac{\mp G_i \cos \kappa^{(i)} (h \pm x_3)}{c^{(i)} \kappa^{(i)}} \quad , \tag{4.45}$$

the constant of integration, amounting to a rigid body translation, is discarded because it does not satisfy (2.39).

From our choices of voltage and current variables and our definition (4.42), we can use (4.43) and (4.45) to obtain the self and mutual mechanical terms.

Straightforward calculation for i = 1 gives

$$V_1^{o} = A\, G_1 \sin \theta_1 \,, \tag{4.46}$$

$$I_1^{o} = -j\omega\, G_1 \cos \theta_1 / (c^{(1)} \kappa^{(1)}) \,, \tag{4.47}$$

so that

$$y_{11}^{o} = \frac{Y_o^{(1)}}{j \tan \theta_1} \quad , \tag{4.48}$$

with the usual definitions. The same arguments we used in the TETM case now can be used to arrive at

$$y_{11}^{\circ} = y_{44}^{\circ} = \frac{Y_o^{(1)}}{j \tan \theta_1}, \tag{4.49}$$

$$y_{22}^{\circ} = y_{55}^{\circ} = \frac{Y_o^{(2)}}{j \tan \theta_2}, \tag{4.50}$$

and

$$y_{33}^{\circ} = y_{66}^{\circ} = \frac{Y_o^{(3)}}{j \tan \theta_3}, \tag{4.51}$$

which completes the determination of the main diagonal terms.

2. From (4.44) we see that only mechanical off-diagonal matrix elements determined by the same mode index number (i) are non-zero, which means that, according to (3.35), (3.36) and (3.38), (3.39), those whose port numbers differ by three.

For example, with (4.46) for V_1°, only I_4° is finite (apart from I_1°, obviously; but this leads to the main diagonal term y_{11}°). For I_4° we obtain,

$$I_4^{\circ} = +j\omega G_1 / (c^{(1)} x^{(1)}), \tag{4.52}$$

leading to

$$y_{41}^{\circ} = \frac{Y_o^{(1)}}{-j \sin \theta_1}. \tag{4.53}$$

Again we use the TEM arguments, about permuting modal index numbers, etc., to deduce

$$y^{\circ}_{14} = y^{\circ}_{41} = \frac{Y_o^{(1)}}{-j \sin \theta_1}, \tag{4.54}$$

$$y^{\circ}_{25} = y^{\circ}_{52} = \frac{Y_o^{(2)}}{-j \sin \theta_2}, \tag{4.55}$$

and

$$y^{\circ}_{36} = y^{\circ}_{63} = \frac{Y_o^{(3)}}{-j \sin \theta_3}. \tag{4.56}$$

Similarly we find that components with the following indices are zero: 12,13,15,16,23,24,26,34,35,45,46 and 56, plus, of course, those on the other side of the diagonal, with the digits in reversed order. This follows from (4.44), as we remarked in the discussion between (4.51) and (4.52).

One set of elements remains to be determined, the electromechanical mutual terms. These are found by application of V_7° and measuring the I_{ξ}° (ξ = 1 to 6). Now we take all T_{3i}° to be zero at the surfaces of the plate, a condition which we encountered in Section A, above. In fact, we can borrow those results, because we know that an applied field E_1 produces the displacements u_i° given by (4.21). We said, in the discussion after (4.27), that E_1 could be looked upon as arising from a potential difference $(-E_1(2\ell))$. If this is our V_7°, appropriate to a portion of the plate of length 2ℓ along x_1, then, by the use of (4.21), (4.23) and (4.32), along with (3.38), (3.39), we can determine $y^{\circ}_{\pi 7}$.

After a simple calculation, and applying our usual methods of

symmetry, etc., we obtain

$$y^{\circ}_{17} = y^{\circ}_{71} = y^{\circ}_{47} = y^{\circ}_{74} = \frac{n_1 \, Y_o^{(1)}}{j \cot(\theta_1/2)}, \tag{4.57}$$

$$y^{\circ}_{27} = y^{\circ}_{72} = y^{\circ}_{57} = y^{\circ}_{75} = \frac{n_2 \, Y_o^{(2)}}{j \cot(\theta_2/2)}, \tag{4.58}$$

and

$$y^{\circ}_{37} = y^{\circ}_{73} = y^{\circ}_{67} = y^{\circ}_{76} = \frac{n_3 \, Y_o^{(3)}}{j \cot(\theta_3/2)}. \tag{4.59}$$

This completes the determination of the admittance matrix, which is written out fully on the next page, the element y°_{77} being given by (4.30).

$$
[y^o] = \begin{bmatrix}
\frac{Y_o^{(1)}}{j\tan\theta_1} & 0 & 0 & \frac{Y_o^{(1)}}{-j\sin\theta_1} & 0 & 0 & \frac{n_1 Y_o^{(1)}}{j\cot(\theta_1/2)} \\
0 & \frac{Y_o^{(2)}}{j\tan\theta_2} & 0 & 0 & \frac{Y_o^{(2)}}{-j\sin\theta_2} & 0 & \frac{n_2 Y_o^{(2)}}{j\cot(\theta_2/2)} \\
0 & 0 & \frac{Y_o^{(3)}}{j\tan\theta_3} & 0 & 0 & \frac{Y_o^{(3)}}{-j\sin\theta_3} & \frac{n_3 Y_o^{(3)}}{j\cot(\theta_3/2)} \\
\frac{Y_o^{(1)}}{-j\sin\theta_1} & 0 & 0 & \frac{Y_o^{(1)}}{j\tan\theta_1} & 0 & 0 & \frac{n_1 Y_o^{(1)}}{j\cot(\theta_1/2)} \\
0 & \frac{Y_o^{(2)}}{-j\sin\theta_2} & 0 & 0 & \frac{Y_o^{(2)}}{j\tan\theta_2} & 0 & \frac{n_2 Y_o^{(2)}}{j\cot(\theta_2/2)} \\
0 & 0 & \frac{Y_o^{(3)}}{-j\sin\theta_3} & 0 & 0 & \frac{Y_o^{(3)}}{j\tan\theta_3} & \frac{n_3 Y_o^{(3)}}{j\cot(\theta_3/2)} \\
\frac{n_1 Y_o^{(1)}}{j\cot(\theta_1/2)} & \frac{n_2 Y_o^{(2)}}{j\cot(\theta_2/2)} & \frac{n_3 Y_o^{(3)}}{j\cot(\theta_3/2)} & \frac{n_1 Y_o^{(1)}}{j\cot(\theta_1/2)} & \frac{n_2 Y_o^{(2)}}{j\cot(\theta_2/2)} & \frac{n_3 Y_o^{(3)}}{j\cot(\theta_3/2)} & y^o_{77}
\end{bmatrix}
$$

D. The Electromechanical Network Admittance Matrix.

Having obtained the admittance matrix from the mathematical statement of the physical problem, we wish here to synthesize a transmission-line network that realizes this same matrix exactly, and, further, one that can be shown to be a true analog of the vibrating plate, in the normal coordinate system. The results of the next chapter will then provide the necessary additional circuitry to complete the development of true analogs for a single plate, and, at the same time, lead naturally, in Chapter VI, to generalizations of our results wherein any number of layers may be accommodated by our representations.

1. We may shorten the procedure of finding an appropriate network by considering our past results, particularly Fig. 13 and Fig. 17. Taken together, they strongly suggest that a circuit identical to that of Fig. 13, but lacking the negative capacitor, will meet the necessary conditions. And so, we consider, provisionally, the network of Fig. 20, which has those characteristics we have repeatedly stressed: three modal transmission lines and boundary-forcing, piezoelectric transformers.

One might go to more elaborate lengths to show why the admittance matrix leads to this figure, but it will save space to turn the process around, and simply analyze the conjectured configuration shown.

To this end, we replace each transmission line by its equivalent lumped circuit; shown in Fig. 21, this has been taken in the pi form, which is proper to an admittance determination. The complete seven-port, lumped, network is given in Fig. 22. The port voltage and current conventions are identical with those of Fig. 15. Element

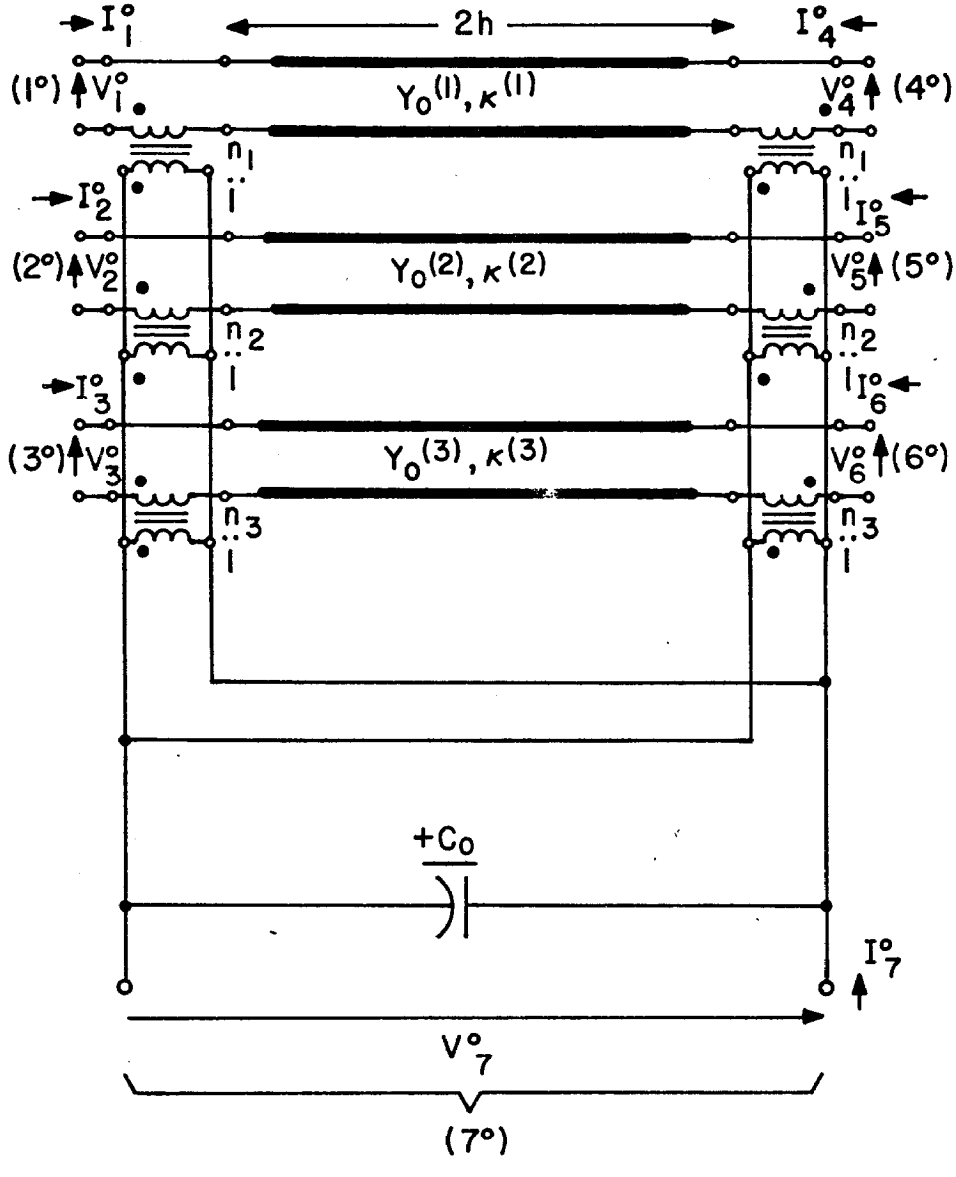

FIG. 20. SEVEN-PORT, NORMAL-MODE, LETM EQUIVALENT CIRCUIT, WITHOUT MECHANICAL BOUNDARY NETWORK AND LOADS.

$$Y_1 = \frac{Y_0}{j \sin\theta} (\cos\theta - 1) = j\, Y_0 \tan(\theta/2)$$

$$Y_2 = \frac{Y_0}{j \sin\theta} \quad ; \quad \theta = \kappa\ell$$

FIG. 21. LUMPED, PI, FORM OF A TRANSMISSION - LINE SECTION

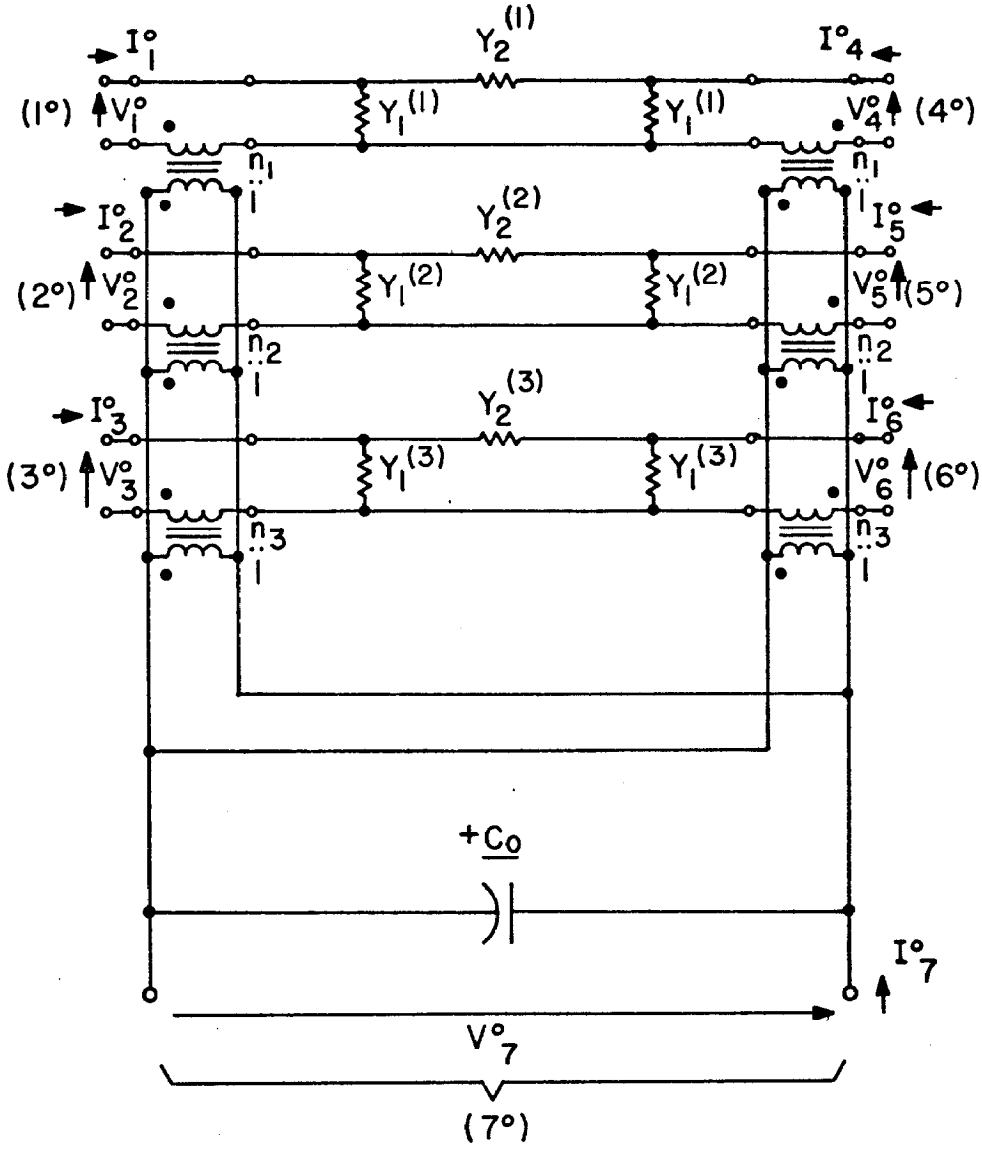

FIG. 22. LUMPED CIRCUIT FOR EVALUATING LETM ELECTROMECHANICAL ADMITTANCE MATRIX.

values for the members of the pi circuits are to be taken from Fig. 21, with the necessary sub- or superscripts, relating to the mode number, added.

What remains of our task is simplified, as it was in Section C, by the decoupling effect of the short circuit applied to port (7°). Using elementary circuit analysis, and the inherent symmetries present, we may write down the elements almost by inspection. They are:

$$y_{11}^{\circ} = y_{44}^{\circ} = Y_1^{(1)} + Y_2^{(1)} = \frac{Y_o^{(1)}}{j \tan \theta_1}, \tag{4.60}$$

$$y_{22}^{\circ} = y_{55}^{\circ} = Y_1^{(2)} + Y_2^{(2)} = \frac{Y_o^{(2)}}{j \tan \theta_2}, \tag{4.61}$$

$$y_{33}^{\circ} = y_{66}^{\circ} = Y_1^{(3)} + Y_2^{(3)} = \frac{Y_o^{(3)}}{j \tan \theta_3}. \tag{4.62}$$

To find the term y_{77}°, from the circuit given, it is easiest to resort to a bisection, as was done to obtain Fig. 19. The situation is the same, because ports (1°) to (6°) are now shorted, as in the former case. As no current flows through the three series arms, denoted as $Y_2^{(i)}$ in the figure, because of symmetry, they are bisected with an open circuit, and the result is three pairs of admittances in parallel, that are seen on the primary sides of the transformers as a total admittance of value

$$2 \cdot \sum_{i=1}^{3} n_i^2 \, Y_1^{(i)} \, . \tag{4.63}$$

When the admittance of Co is added to this, and we use, from Fig. 21,

$$Y_1^{(i)} = j \, Y_o^{(i)} \tan(\theta_i/2), \tag{4.64}$$

we get

$$y_{77}^{o} = j\omega C_o + j2 \sum_{i=1}^{3} n_i^2 \, Y_o^{(i)} \tan(\theta_i/2). \tag{4.65}$$

By using the definitions of Co, $n_i Yo^{(i)}$ and θ_i, this may be put into the form (4.30), the required result.

The finite mechanical mutual terms are simply the negative of the series arm of the proper pi, so that we have

$$y_{14}^{o} = y_{41}^{o} = -Y_2^{(1)} = \frac{Y_o^{(1)}}{-j \sin\theta_1}, \tag{4.66}$$

$$y_{25}^{o} = y_{52}^{o} = -Y_2^{(2)} = \frac{Y_o^{(2)}}{-j \sin\theta_2}, \tag{4.67}$$

$$y_{36}^{o} = y_{63}^{o} = -Y_2^{(3)} = \frac{Y_o^{(3)}}{-j \sin\theta_3}, \tag{4.68}$$

while it is seen, by inspection, that the terms subscripted 12,13,15, 16,23,24,26,34,35,45,46, and 56, are zero, as are the corresponding terms below the diagonal.

The remaining category is that of the electromechanical mutual terms; these are found by forcing with V_7^o . Symmetry was used to get y_{77}^o , and it is useful here also. We use the same bisection as previously, but reason that the full voltage appears across each transformer, so that secondary voltages of $n_i V_7^o$ serve as the sources in each of six simple loops, each consisting only of $Y_1^{(i)}$, producing currents of $n_i Y_1^{(i)}$, circulating, in every case, in the direction counter to the particular port current I_ξ^o ; thus the admittance elements are equal to

$$-n_i Y_1^{(i)} = \frac{n_i Y_o^{(i)}}{j \cot(\theta_i/2)} . \tag{4.69}$$

In particular

$$y_{17}^o = y_{47}^o = \frac{n_1 Y_o^{(1)}}{j \cot(\theta_1/2)} , \tag{4.70}$$

$$y_{27}^o = y_{57}^o = \frac{n_2 Y_o^{(2)}}{j \cot(\theta_2/2)} , \tag{4.71}$$

$$y_{37}^o = y_{67}^o = \frac{n_3 Y_o^{(3)}}{j \cot(\theta_3/2)} , \tag{4.72}$$

which, with the symmetry $y_{\pi\xi}^o = y_{\xi\pi}^o$ completes the evaluation. We see the results are in accordance with what we obtained from the equations of the plate, so the network of Fig. 20 represents the physics of the problem, insofar as may be seen from the seven ports (π^o).

2. That the network of Fig. 20 actually does more than represent the physical situation at the seven ports may be shown by following the

argument as we gave it in Section III E. The stresses are given by (4.16) instead of (2.38), with $-\overset{\circ}{e}_{13i} E_1$ suffering a discontinuity at the surface instead of $\overset{\circ}{e}_{33i} a_3$, but the conclusion remains unaltered: the placing of the piezo-transformers at the boundaries has this definite significance, as explained. The discussion regarding the identification of the transmission line variables with the plate mechanical voltages and currents is likewise unchanged, and therefore, quite simply, we have established that Fig. 20 is a true analog of the physical problem of the LEIM-driven crystal plate, up to the boundaries.

A consideration of the situation at the boundaries is the subject for discussion in the next chapter. There we will obtain additional circuitry to place at the normal coordinate ports (π°) to complete the physical and network pictures.